DIFFERENTIAL DIAGENESIS OF RHYTHMIC LIMESTONE ALTERNATIONS SUPPORTED BY PALYNOLOGICAL EVIDENCE

HILDEGARD WESTPHAL,[1]* MARTIN J. HEAD,[2]** AND AXEL MUNNECKE[3]†

[1] *Comparative Sedimentology Laboratory, University of Miami, RSMAS, 4600 Rickenbacker Causeway, Miami Florida 33149-1098, U.S.A.*
e-mail: hwestphal@mbox.geowi.uni-hanover.de
[2] *Department of Geology, University of Toronto, 22 Russell Street, Toronto, Ontario, M5S 3B1, Canada*
[3] *Institut für Geowissenschaften, Universität Kiel, Olshausenstraße 40-60, 24118 Kiel, Germany*

ABSTRACT: Alternating cemented and uncemented, fine-grained layers from Pliocene periplatform carbonates of the Great Bahama Bank have fundamentally different diagenetic features. The cemented layers consist predominantly of microspar, interpreted as an early marine, shallow-burial cement. The intercalated, uncemented, softer layers are devoid of microspar cement and exhibit signs of mechanical compaction. Precursor sediments of both cemented and uncemented layers apparently consisted largely of aragonite needles. The needles in the compacted layers show signs of dissolution, suggesting that the calcium carbonate required for cementation of the uncompacted layers was provided by aragonite dissolution within the compacted layers. The lack of compaction in the cemented layers shows that cementation, and hence aragonite dissolution in the adjacent compacted layers, took place in the shallow-burial realm. The dissolved carbonate was transported by diffusion to adjacent layers and reprecipitated as calcite cement, thereby preventing significant compaction of these layers. These processes are not yet complete in the material examined, and some aragonite remains in the compacted layers.

The sedimentary composition of the two rock types (compacted and uncompacted) is similar, indicating a similar precursor sediment for both. Between 1.5 and 7 times the concentration of palynomorphs occurs in the compacted layers, apparently the result of passive diagenetic enrichment. Although the trigger for diagenetic differentiation has not been determined, the pure limestone succession studied here appears to serve as a clay-free analog to limestone–marl alternations.

INTRODUCTION

''The central difficulty is tantalisingly familiar—how to cement a carbonate mud while it is still largely uncompacted. . . . Where was the source of such an enormous quantity of CaCO₃ . . . ?'' (Bathurst 1970, p. 430). The source of the carbonate cement lithifying uncompacted fine-grained limestones remains one of the crucial problems in carbonate sedimentology (Bathurst 1971; Steinen 1982; Morse and Mackenzie 1993). The common occurrence of such uncompacted fine-grained limestones throughout the geologic record requires early diagenetic import of carbonate cement. This imported calcium carbonate occludes the primary pore space and produces a rigid framework prior to the accumulation of sedimentary overburden that could compact the sediment (Bathurst 1970).

Uncompacted fine-grained limestones are well known, e.g., from many limestone–marl alternations of various ages and locations (Einsele and Ricken 1991). In limestone–marl alternations the uncompacted limestones are separated by marl beds that typically are strongly compacted. In such alternations, it has been postulated that the carbonate cement filling the primary pore space of the uncompacted limestones was derived from these intercalated marl beds (Eder 1982; Ricken 1986; Munnecke and Samtleben 1996; Munnecke 1997).

Alternations of cemented and uncemented layers occur also in pure carbonate systems such as the Bahamian periplatform carbonate successions (Dix and Mullins 1988a; Schlanger and Douglas 1974), where the mechanisms of diagenetic differentiation are especially enigmatic. The segregation of cemented and uncemented layers in periplatform carbonates could be caused by differences in the diagenetic potential, i.e., differences in the proportion of metastable phases of calcium carbonate and/or organic matter in the original sediment, or differences in reactive surface areas of the sediment, by fluctuations of the carbonate compensation depth, or by varying sedimentation rates (Schlanger and Douglas 1974; Dix and Mullins 1988a). However, in initially metastable carbonate sediments the primary sediment composition is usually disguised during diagenesis by selective dissolution (e.g., of aragonitic components) and by recrystallization. Therefore, in fossil carbonates, present-day differences in carbonate content as well as in sedimentary components and trace elements do not necessarily reflect primary differences (Bathurst 1987).

This study aims to contribute to this discussion by (1) using palynomorph assemblages and concentrations as indicators of stability in the sedimentary input and by (2) proposing a model for an early diagenetic differentiation into cemented and uncemented layers.

GEOLOGIC SETTING

The western, leeward slope of the Great Bahama Bank is characterized by low-angle, prograding clinoforms of Tertiary and Quaternary age (Eberli and Ginsburg 1987, 1989; Eberli et al. 1997). Borehole Clino was drilled in a water depth of 7.60 m at the present margin of the Great Bahama Bank (Figs. 1, 2; Ginsburg in press). It penetrated a series of inclined seismic reflectors that represent slope deposits beneath a thin Upper Pleistocene and Holocene platform succession (Eberli et al. 1997). Clino recovered a succession of Neogene slope sediments and terminated in Upper Miocene deposits at 677.27 m below mud pit (mbmp; mud pit was 7.30 m above sea level).

The Clino core consists of a shallowing-upward slope succession of almost pure periplatform carbonates. Most samples contain about 1 wt % insoluble residue, about one-third of this being organic (Kenter et al. in press). Fine-grained intervals (mud- to silt- and fine sand-size grains) dominate, with thin intercalated, coarser-grained beds (Fig. 3; Kenter et al. in press; Melim et al. in press b). By far the dominant fine-grained sedimentary constituents are aragonite needles of up to 10 μm in length. In the fine-grained intervals, the matrix makes up about 50 vol % of the sediment in the Lower Pliocene and about 70 vol % in the Upper Pliocene, in some samples exceeding 90 vol % (Westphal 1998). Coarser components include peloids, foraminifers, ostracodes, and *Halimeda* plates. The coarse-grained beds are interpreted as gravity-flow deposits during sea-level lowstands, whereas the fine-grained layers are thought to represent off-bank sedimentation from suspension during highstands (Westphal et al. 1999; Kenter et al. in press; Melim et al. in press b). The present study reports on fine-grained sediment from a section in the Lower Pliocene (476.40–494.39 mbmp) and a section in the Upper Pliocene (220.48–262.18 mbmp; Fig. 3). The depositional depth of these intervals is thought to have exceeded 300 m for the Lower Pliocene and 200 m for the Upper Pliocene, which is below the influence of meteoric diagenesis (Melim et al. 1995; Melim 1996).

* Present address: Geologisches Institut, Universität Hannover, Callinstr. 30, 30167 Hannover, Germany.
** Present address: Godwin Institute for Quaternary Research, Dept. of Geography, University of Cambridge, Downing Place, Cambridge CB2 3EN, UK.
† Present address: Institute für Geologie und Paläontologie, Universität Tübingen, Herrenberger Str. 51, 72070 Tübingen, Germany.

Fig. 1.—Location of borehole Clino of the Bahamas Drilling Project and seismic "Western Geophysical Line", Great Bahama Bank. Borehole Clino is located on the present leeward platform margin. TOTO = Tongue of the Ocean. (From Eberli et al. 1997.)

The degree of lithification in the Pliocene of the Clino core does not increase linearly with burial depth (Melim et al. in press b; Westphal 1998). The fine-grained intervals upon which this study focuses are characterized by an irregular succession of cemented and uncemented layers. The uniformly light-tan nature and fine grain size of the sediments makes it difficult to estimate the compaction on the basis of macroscopic core descriptions. The columns to the right in Figure 3 show the succession of compacted versus uncompacted layers as determined from grain deformation (mostly peloids) in thin sections. The thickness of the compacted and uncompacted layers as apparent from thin sections varies from 6 cm to 2.40 m, where 6 cm is the shortest sampling interval (sampling distance was normally 15 cm for the Lower Pliocene and 30 cm for the Upper Pliocene). The average layer thickness for the Lower Pliocene succession is 0.27 m for the compacted and 0.37 m for the uncompacted layers, and for the Upper Pliocene the average thickness is 0.56 m for the compacted layers and 0.73 m for the uncompacted layers. The proportion of compacted layers is about 40% for both intervals. Aragonite contents range from 0% to 34% (average 16%) in the Lower Pliocene and from 33% to 85% (average 57%) in the Upper Pliocene (Fig. 4; XRD data from Westphal 1998). In both intervals, samples

from the compacted layers show slightly higher aragonite contents than the uncompacted layers (averages for Lower Pliocene, 19 wt % versus 14 wt %; averages for Upper Pliocene, 62 wt % versus 49 wt %; Fig. 4). Porosities average 37.0% for the Lower Pliocene interval and 38.2% for the Upper Pliocene and show no systematic relationship with the alternation of compacted and uncompacted layers (Fig. 3; porosity data by the Comparative Sedimentology Laboratory, Miami).

The intervals examined cover time spans of roughly 200 kyr and 100 kyr for the Lower and Upper Pliocene, respectively (Westphal 1998; calculation based on Lidz and McNeill 1995). Calculated frequencies would be about 5 ka and 15 ka for the cemented–uncemented couplets in the Lower and Upper Pliocene intervals, respectively. A marine, shallow-burial diagenetic environment is indicated by the isotopic signature of the cements (Melim et al. 1995; in press b) and by petrography (Melim et al. 1995; Munnecke et al. 1997; Westphal 1998).

METHODS

Petrographic examinations have been carried out mainly with the scanning electron microscope (SEM), supported by light-microscopic obser-
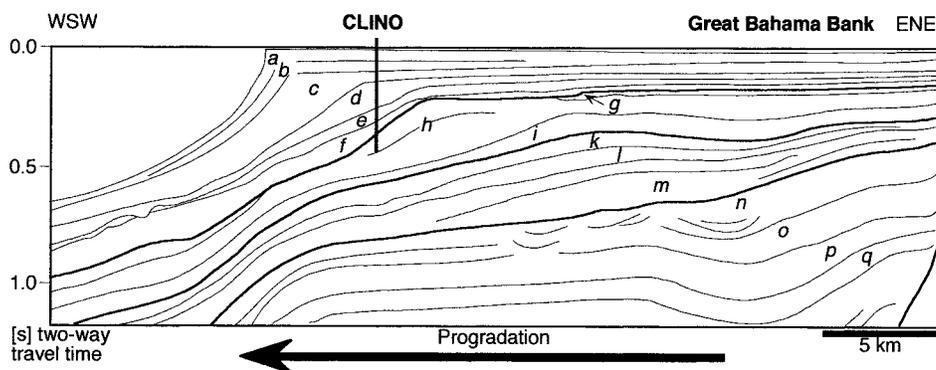
Fig. 2.—Traces of seismic reflections of part of the "Western Geophysical Line" showing the leeward clinoforms that prograde westward. The borehole Clino of the Bahamas Drilling Project penetrates the Miocene (*i* and *h*) to Holocene (*a*) prograding succession of slope sediments. Intervals selected from Clino for the present study are in seismic sequences *f* and *d*. (From Eberli et al. 1997.)

TABLE 1.—*Palynomorph assemblages determined in 12 fine-grained Pliocene samples from the core Clino. Sample pairs indicate those samples taken from adjacent compacted/uncompacted horizons.*

Age	UPPER LOWER PLIOCENE (3.6–4.1 Ma)						UPPER UPPER PLIOCENE (ca. 2.1–2.3 Ma)					
Depth (feet below mud pit)	1622.00	1621.50	1567.50	1565.08	1563.67	1563.00	860.17	858.50	839.50	768.13	763.50	741.50
Depth (meters below mud pit)	494.39	494.23	477.77	477.04	476.61	476.40	262.18	261.67	255.88	234.12	232.71	226.01
compacted?	yes	no	yes	no	yes	no	yes	no	yes	no	yes	no
sample pairs?	sample pair		sample pair		sample pair		sample pair			sample pair		
Dinoflagellates (raw counts)												
Impagidinuim sp. A			+									
Operculodinium janduchenei			+									
Hystrichokolpoma rigaudiae	+	1	+		+	+						
Operculodinium? longispinigerum	1		+	1	1	+						
Bitectatodinium tepikiense s.s.						1						
Impagidinium paradoxum						+		+				
Operculodinium? megagranum									2			
Lejeunecysta marieae									+			
Nematosphaeropsis rigida									4			
Protoperidinioid cyst sp. A									+			
Bitectatodinium cf. *raedwaldii*									+	+		
Operculodinium psilatum	+	+									+	
Bitectatodinium raedwaldii			+	+	+	+	+	3	+		+	
Selenopemphix nephroides	+			+					+	+		+
Selenopemphix quanta	2	+	+	+	+		2	1	1	+	1	+
Tuberculodinium vancampoae	+	+	2	1	2	1				1		3
Ataxiodinium zevenboomii			1				+	+	+	+		(+)?
Melitasphaeridium choanophorum									10	17	6	1
Achomosphaera/Spiniferites spp. (total)	109	42	175	131	139	86	162	137	136	151	173	159
Capisocysta lata	+	+	3	8	2	5	13	11	1	35	15	29
Dapsilidinium pseudocolligerum	2	2	1		+		1	3	3	6	4	10
Kallosphaeridium sp.	*	*	*	*	*	*	*	*	*	*	*	*
Lingulodinium machaerophorum	16	33	5	18	15	13	42	56	77	28	33	25
Operculodinium bahamense	+			+	+	+	+	3	3	+	1	5
Operculodinium spp. including *O. israelianum*	12	9	24	32	42	24	29	33	9	9	11	16
Polysphaeridium zoharyi	104	160	33	47	49	116	+	+	4			
Round brown cysts	4	3	6	12		4	1	3	+	3	6	2
Spiniferites mirabilis	*		*	*	*	*	*	*	*	*	*	
Spiniferites rhizophorus	*	*	*	*	*	*	*	*	*	*	*	*
Lejeunecysta sp. cf. *L. marieae*												
TOTAL IN-SITU DINOFLAGELLATES	250	250	250	250	250	250	250	250	250	250	250	250
Marine algae incertae sedis (raw counts)												
Incertae sedis sp. A			1	+								
Incertae sedis sp. B						+						
Leiospheres	*	*	*	*	*	*	*	*	*	*	*	*
Nanobarbophora walldalei	18	5	32	52	51	14	3	29	1	44	9	19
Small spiny acritarchs	43	11	158	131	112	93	43	108	68	63	51	23
Acritarch sp. 1							*					*
Cyclopsiella sp.									1			
Other marine palynomorphs (raw counts)												
Trochospiral microforaminiferal lining B						*				*		
Copepod fragments		1							+		+	
Foraminiferal linings (6 or more chambers)	11	22	31	19	31	34	9	15	12	9	6	10
Scolecodonts	1		1	2		4						
Terrestrial palynomorphs (raw counts)												
Fungal spores and hyphae									1			
Fern and bryophyte spores					1			1	1		+	
Bisaccate pollen	1	4	1	1				4	6	2	2	3
Angiosperm pollen		1		1		1			3			+
TOTAL TERRESTRIAL PALYNOMORPHS	1	5	1	2	1	1	0	5	11	2	2	3
Terrestrial palynomorphs/dinoflagellates	0.004	0.020	0.004	0.008	0.004	0.004	0.000	0.020	0.044	0.008	0.008	0.012
Sample data												
Sample dry weight (in grams)	8.6	2.1	3.5	13	14.3	10.4	8	3.9	5.9	18.6	2.2	3.2
Quantity of *Lycopodium clavatum* tablets	1	1	1	2	2	1	1	1	1	3	1	1
Quantity of *Lycopodium clavatum* spores counted	27	325	94	90	35	173	95	278	241	176	117	605
Palynomorphs per gram dry weight (concentrations)†												
Estimated total dinoflagellates	**15,000**	**5,100**	**10,600**	**5,900**	**13,900**	**1,900**	**4,600**	**3,200**	**2,400**	**3,200**	**13,500**	**1,800**
(estimated standard error)	(±3,100)	(±500)	(±1,400)	(±800)	(±2,600)	(±200)	(±600)	(±300)	(±300)	(±300)	(±1,700)	(±200)
Estimated total terrestrial palynomorphs	60	102	42	48	56	8	0	64	108	25	108	22
(estimated standard error)	(±61)	(±46)	(±42)	(±34)	(±57)	(±8)	(±0)	(±29)	(±34)	(±18)	(±77)	(±13)

Note the absence of systematic differences in the assemblages between compacted and uncompacted samples. The absolute numbers of palynomorphs present, however, is distinctly higher in compacted samples. Adapted and slightly modified from Head and Westphal (1999, Fig. 3). Asterisk indicates "present but not enumerated during counts". Cross indicates "recorded only outside of counts". † = Figures rounded to nearest 100.

vations. The present study describes these qualitative observations. A detailed quantitative component analysis of the studied intervals is given in Westphal (1998). For petrographic SEM analyses, rock samples were cut perpendicular to bedding and polished with corundum powder 2000. Polished samples were etched for 20 seconds in 0.1 molar hydrochloric acid and coated with gold/palladium. The etching process produces a relief that accentuates the crystal boundaries and insoluble constituents. Stereoscopic pairs of SEM micrographs (with an angle of 6° between micrographs) were used to examine the three-dimensional shape of constituents.

For the palynological investigations, samples were weighed and then

Clino

margin-reef-platform

late Pliocene - Pleistocene

upper slope

early Pliocene

lower slope

late Miocene

mbmp

Upper Pliocene

mbmp   M W P G
Dunham Classification

Lower Pliocene

mbmp   M W P G
Dunham Classification

u/c   c   % porosity

u/c   c

lithology:

peloidal-skeletal packstone to mudstone

coral boundstone

skeletal (reefal) packstone to rudstone

peloidal packstone to grainstone (< 150 μm)

peloidal packstone to wackestone (< 250 μm)

skeletal and/or foraminiferal packstone to grainstone (> 125 μm)

skeletal-peloidal packstone to grainstone (> 250 μm)

peloidal-skeletal packstone to grainstone (> 250 μm)

demineralized using cold HCl and HF in order to free the organic component. Neither oxidants, alkalis, nor hot acids were used, because these can damage organic-walled microfossils, particularly the cysts of certain heterotrophic dinoflagellates. The organic residue was then briefly subjected to ultrasound (30–45 s) to disperse unwanted organic matter prior to sieving. Tablets containing a known quantity of *Lycopodium clavatum* spores were added to a given amount of sediment as a standard in order to facilitate the determination of absolute abundances per gram dry weight of sediment (see Stockmarr 1971; Maher 1981). The determination is based on the observed ratio of *Lycopodium clavatum* spores to indigenous palynomorphs, and saves having to count every palynomorph in the sample. The method also corrects for any small losses during processing (*Lycopodium clavatum* spores would be lost by the same proportion as indigenous palynomorphs). These commercially available spores are popular as marker grains because they are easily recognized under the microscope by their dark coloration (the result of being acetolyzed by the manufacturers of the tablets) and distinctive morphology. Microscope slides were made using residues sieved at >10 μm for the quantitative study of dinoflagellate cysts and other palynomorphs. Where available, remaining residue was sieved at >20 μm and mounted on microscope slides to concentrate the larger dinoflagellate cysts. This made it possible to search effectively for any rare specimens present in the sample.

PETROGRAPHY

Cemented Layers

Fecal pellets, burrows, and delicate, thin-walled organic microfossils are all undeformed in the cemented layers. These layers contain cloudy microspar with abundant inclusions (Fig. 5A). Calcitic microfossils such as foraminifers are typically well preserved. Under SEM, the layers show a dense mosaic of low-Mg calcite crystals (mostly microspar; Fig. 5B). The sharp boundaries between cement crystals and calcitic components such as foraminifer tests show that only minor recrystallization has taken place. Aragonite needles are typically engulfed in the microspar crystals and are responsible for the cloudy appearance of the microspar under the light microscope (Fig. 5D). In a number of samples aragonitic constituents were dissolved, leaving molds. In these samples, microspar crystals contain needle-shaped pits of about 1 μm in diameter and several μm in length.

Uncemented Layers

Macroscopically, the intercalated softer layers are commonly distinguished by compaction features such as strongly deformed pellets and burrows, although these structures sometimes appear rather faint because of the generally light color of these carbonates. In the core slabs, compaction produces the appearance of lamination. This alignment of elongated constituents is also observed in thin section (Fig. 5E). Locally, mineralized microfossils, such as delicate foraminifer tests, are broken. The dense mosaic of microspar crystals, characteristic of uncompacted layers, is absent in the compacted layers. Instead either a dense mesh of aragonite needles (Fig. 5F$_1$) or a micritic matrix of non-fitted crystals dominates (Fig. 5F$_2$). Aragonite needles show dissolution features (Fig. 5H). Organic microfossils such as dinoflagellate cysts are flattened and typically align with the diagenetic lamination (Fig. 5G).
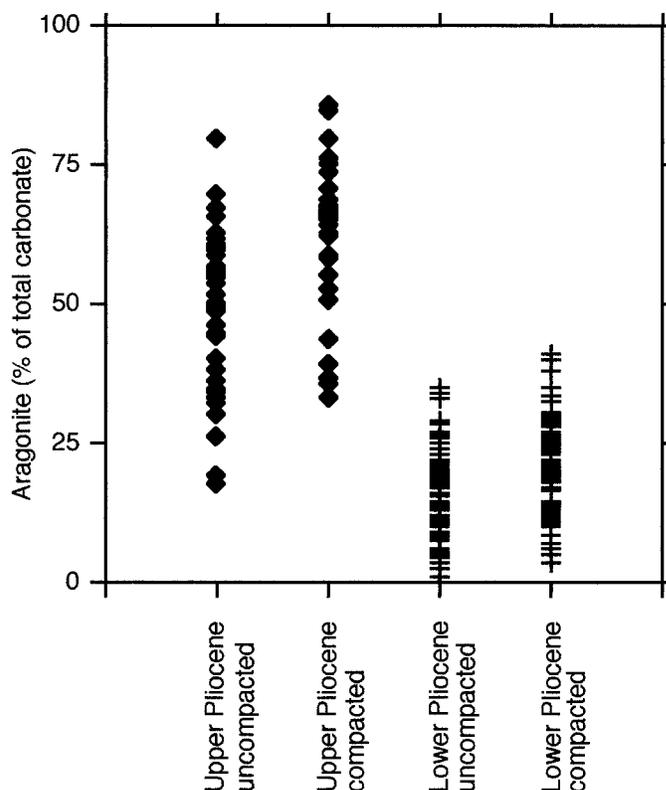
FIG. 4.—Aragonite contents in fine-grained samples from the Upper and Lower Pliocene intervals in Clino split between populations of compacted and uncompacted samples. Note the higher aragonite contents in the compacted samples.

PALYNOLOGY

Assemblages contain abundant dinoflagellate cysts, acritarchs, foraminiferal linings, and rare pollen, spores, and terrestrial debris. These palynomorphs are diagenetically inert (Lind and Schiøler 1994), and preservation varies from fair to excellent. *In situ* examinations of organic-walled dinoflagellate cysts in polished bulk-rock SEM samples have shown that the preservation of these originally spherical cysts varies between cemented and uncemented layers. In cemented layers, most cysts show their original spherical shape, whereas cysts in the compacted layers are always deformed (Fig. 5C, G).

The dinoflagellates are dominated by neritic species, whereas oceanic species are rare. Many of the species have tropical to warm temperate affinities, and several are euryhaline. The assemblages have low species diversity (Table 1), although there is some distinction between the Lower and Upper Pliocene intervals. A selection of characteristic dinoflagellates is illustrated in Figure 6. For a detailed description of the palynomorph species and their environmental significance, the reader is referred to Head and Westphal (1999).

Lower Pliocene

The taxonomic composition of palynomorph assemblages in cemented layers is not significantly different from that of uncemented layers. In con-

←

FIG. 3.—Left column: Lithology of core Clino, showing a general shallowing-upward trend from lower slope to platform-top sediments (after Kenter et al. in press). The intervals examined for this study are highlighted with gray and are shown enlarged in the second column (from Westphal 1998). The third columns show the compacted versus uncompacted preservation of the succession (indicated as ''c'' and ''u/c'', respectively) as determined from thin sections (mainly peloid deformation; each point is a petrographic sample). Arrows indicate position of palynologic samples. To the right, porosity data are shown (data from Melim et al. in press a).
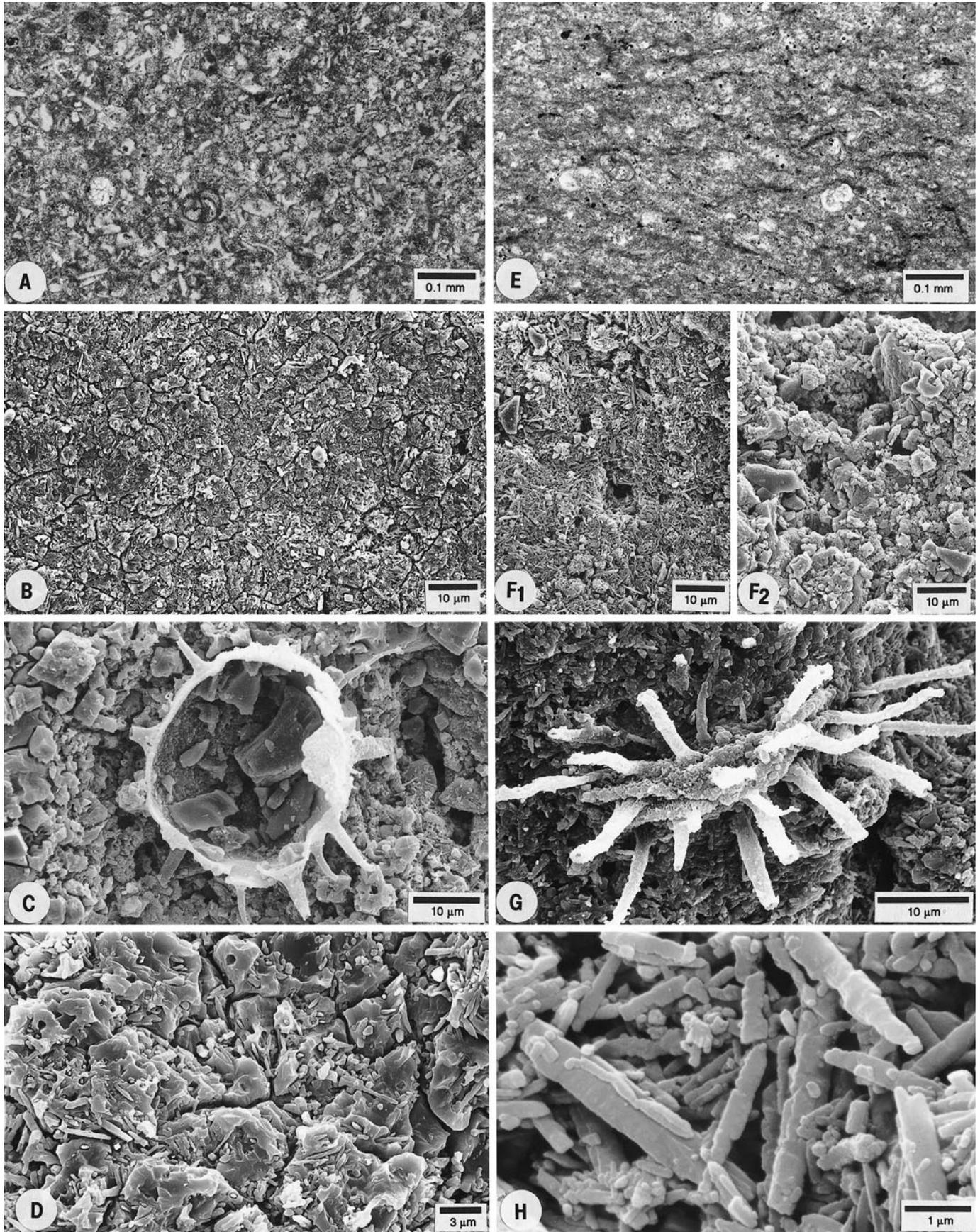
trast, the concentrations of dinoflagellate cysts vary consistently between cemented and uncemented layers (Fig. 7, Table 1). In uncemented layers the concentration of dinoflagellate cysts varies between 10,600 and 15,000 per gram dry sediment, whereas in cemented layers this value varies between 2000 and 6000. In sample pairs from adjacent layers (Table 1), concentrations in compacted samples always exceed those of the adjacent cemented layer, with up to seven times as many dinoflagellate cysts occurring in the compacted sample (sample pair 476.61 mbmp and 476.40 mbmp, 13,897 versus 1933 cysts per gram dry sediment).

Upper Pliocene

The Upper Pliocene palynomorph assemblages are more variable taxonomically than in the Lower Pliocene interval, but this variability does not appear related to cementation. However, dinoflagellate cyst concentrations do vary depending upon whether the layers are cemented or not. Hence the compacted layers contain 2400 to 13,500 dinoflagellate cysts per gram dry sediment whereas the uncompacted layers have 1800 to 3200 cysts.

The distinct difference in concentration of dinoflagellate cysts between compacted and uncompacted layers is more obvious for the Lower Pliocene data set than for the Upper Pliocene, because in the Lower Pliocene (1) the spacing between the sample pairs is tighter, and (2) the underlying longer-term environmental changes recorded in the sediments are less pronounced in this Lower Pliocene interval (Westphal et al. 1999).

DISCUSSION

To address the fundamental question regarding the source of cement in the uncompacted samples (Bathurst 1970, p. 430), we need to examine closely the striking pattern of alternating cemented/uncemented layers. From calculations of reaction kinetics, Morse and Mackenzie (1993) suggest a close spatial relationship between dissolution and reprecipitation of calcium carbonate (''donor limestones'' and ''receptor limestones'' of Bathurst 1971). Therefore, especially in fine-grained sediments, with their low initial permeability (Enos and Sawatsky 1981), the source of the cement should be located within the sedimentary succession itself, and a local redistribution of the calcium carbonate is expected.

In the uppermost few meters of the sedimentary column the primary pore space in fine-grained carbonates typically exceeds 70% or even 80% (Goldhammer 1997; Enos and Sawatsky 1981). A strong reduction in thickness to about 50% of the original thickness can occur at burial depths of less than 150–200 m (Goldhammer 1997). The absence of compaction from many of the initially highly porous layers of the Pliocene periplatform succession requires an external source of carbonate cement to infill the primary pore space and create a rigid framework prior to mechanical compaction. The volumetric increase of 8.0–8.7% that accompanies the *in situ* transformation of aragonite to calcite (Schmidt 1965; Pingitore 1970) within the cemented layers cannot supply sufficient volume of carbonate cement to completely infill the primary pore space. Circulating seawater as a source for the carbonate cement is also unlikely because of the huge volume of water required to provide the dissolved calcium carbonate (Enos and Sawatsky 1981). Marine diagenesis on the sea floor is characterized by the

formation of hardgrounds. In the successions examined, however, the majority of limestone beds are not associated with hardground-related features such as, e.g., boring surfaces and phosphate precipitates, and thus marine sea-floor diagenesis appears to be insignificant.

If we assume a local redistribution of calcium carbonate within the succession as the dominant mechanism for the early diagenetic alteration of the periplatform sediments, then an insoluble reference is needed to test this idea. It has already been shown that within the Lower Pliocene interval as well as within the Upper Pliocene interval there are no substantial differences in the dinoflagellate assemblage composition or of the palynofacies as a whole. It can therefore be suggested that cyst input was relatively constant during sedimentation, allowing the use of cysts as an independent reference. A similar approach has been used by Lind and Schiøler (1994) for assessment of dissolution in stylolites. We dismissed clay content as a standard because quantities are too low (less than 1 wt %) to determine whether any fluctuations in clay input resulted from environmental changes.

Dinoflagellate cyst concentrations are up to seven times higher in compacted layers than in adjacent uncompacted layers. This points to passive enrichment of these insoluble, diagenetically inert constituents, a process interpreted as the result of aragonite dissolution followed by export of the dissolved calcium carbonate. Dinoflagellate concentrations show a roughly linear relationship with total organic carbon (TOC) concentrations (Westphal 1998), which supports the interpretation of passive enrichment. The difference in cyst concentrations between cemented and uncemented samples is attributed principally to removal of carbonate from the compacted layers and import of cement into the uncompacted layers.

These observations lead us to a diagenetic model illustrating two different but complementary paths of development: (1) that of uncompacted, calcium-carbonate importer layers (receptor limestones) and (2) that of compacted, calcium-carbonate exporter layers (donor limestones) (Fig. 8):

(1) Calcium-Carbonate Importer Layers

Lack of compaction in the cemented limestone layers, as demonstrated by the spherical preservation of dinoflagellate cysts, implies that cementation occurred early, i.e., before enough sediment overburden accumulated to cause discernible compaction. According to Melim et al. (1995, in press b) lithification took place in a shallow-burial environment. The imported calcium carbonate is precipitated as microspar calcite cement that forms crystals of up to about 30 μm in longest dimension. This microspar encloses small sedimentary constituents such as aragonite needles (Fig. 5D). Where these aragonite needles are dissolved during later diagenesis they leave micrometer-size pits in the microspar crystals (Lasemi and Sandberg 1984).

With increasing cementation the cemented layers resist mechanical compaction even under deeper burial conditions. Although no stylolites are observed in the intervals examined, increasing pressure in a deeper burial environment might later result in chemical compaction (stylolites). The postulated end fabric of the cementation path is a typical microsparitic limestone (Munnecke et al. 1997). Some later post-cementation dissolution of aragonitic constituents is demonstrated by the occasional presence of moldic porosity in the cemented samples.

Fɪɢ. 5.—Light-microscope and scanning-electron-microscope photographs of uncompacted (left) and compacted layers (right). **A**) Thin-section micrographs of a fine-grained sample that lacks clear indications of compaction (Lower Pliocene, 503.99 mbmp). **B**) SEM micrograph of a tight mosaic of microspar cement crystals that engulf aragonite needles (Upper Pliocene, 217.17 mbmp). **C**) SEM micrograph of dinoflagellate cyst *Polysphaeridium zoharyi* in spherical preservation. The cyst is internally hollow, implying that early cementation of the matrix prevented deformation of the organic-walled cyst (Lower Pliocene; 497.89 mbmp). **D**) SEM micrograph showing a detail of microspar with enclosed aragonite needles (Upper Pliocene; 262.18 mbmp). **E**) Thin section micrographs of a fine-grained sample that shows clear indications of compaction such as apparent lamination (Lower Pliocene; 453.24 mbmp). **F**) SEM micrographs of compacted samples. 1) Uncemented aragonite needle mesh from the Upper Pliocene (219.94 mbmp). 2) Micritic, uncemented sample from the Lower Pliocene (479.82 mbmp). **G**) SEM micrograph of deformed dinoflagellate cyst in uncemented sample (Upper Pliocene; 253.14 mbmp). **H**) SEM micrograph of unetched sample showing aragonite needles with dissolution features (Upper Pliocene; 256.79 mbmp).
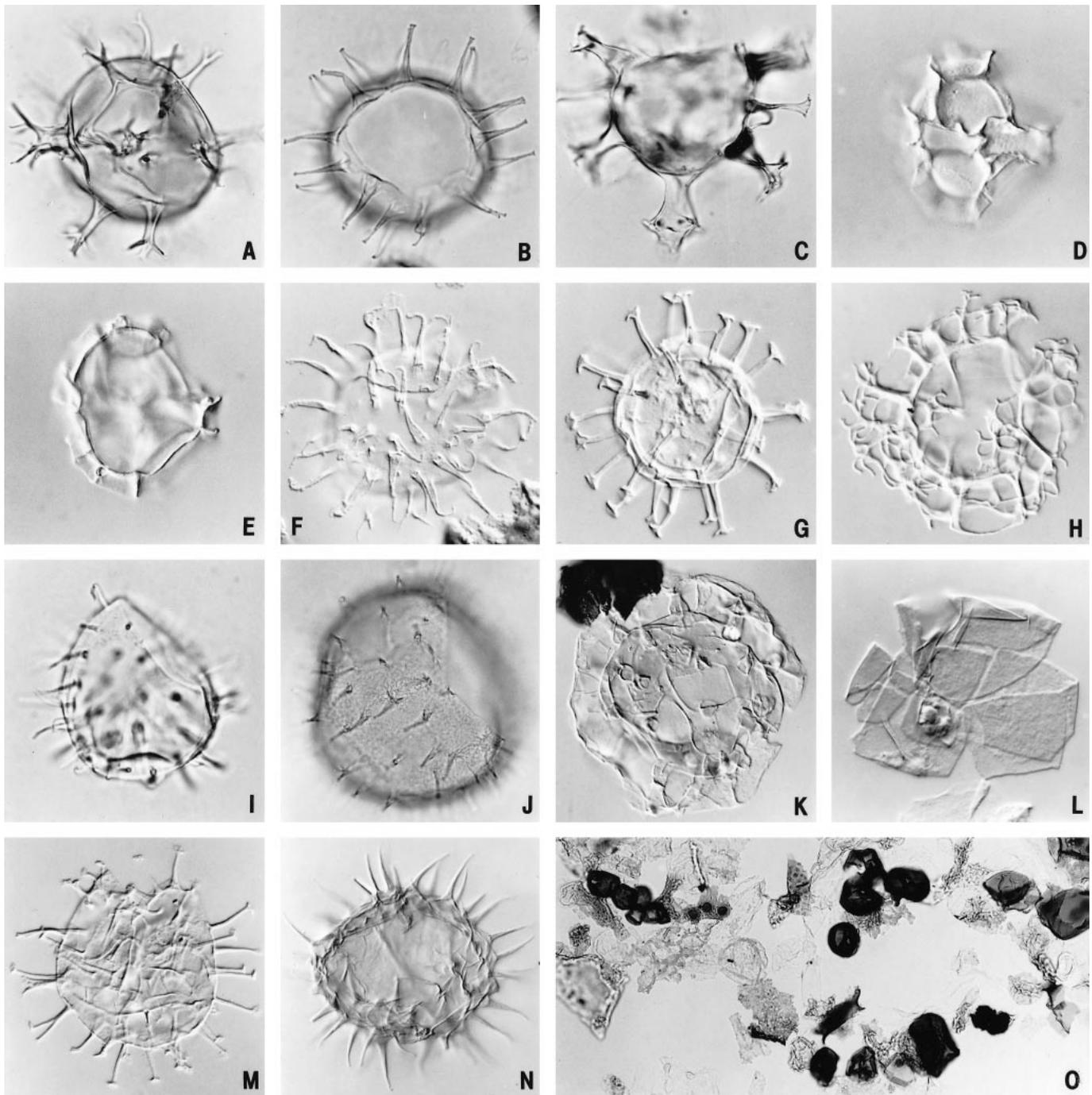
Fɪɢ. 6.—Dinoflagellates and palynofacies of the Clino core. **A)** *Spiniferites rhizophorus* Head *in* Head and Westphal (1999); central body length 48 μm (Lower Pliocene; 476.40 mbmp). **B)** *Dapsilidinium pseudocolligerum* (Stover); central body maximum diameter 42 μm (Upper Pliocene; 232.71 mbmp). **C)** *Hystrichokolpoma rigaudiae* (Deflandre and Cookson); central body width 50 μm (Lower Pliocene; 494.23 mbmp). **D, E)** *Impagidinium paradoxum* (Wall); central body length 32 μm shown at upper and mid foci, respectively (Lower Pliocene; 476.40 mbmp). **F)** *Lingulodinium machaerophorum* (Deflandre and Cookson); central body maximum diameter 46 μm (Lower Pliocene; 476.40 mbmp). **G)** *Melitasphaeridium choanophorum* (Deflandre and Cookson); central body maximum diameter 31 μm (Upper Pliocene; 234.12 mbmp). **H)** *Nematosphaeropsis rigida* Wrenn; central body length 38 μm (Upper Pliocene; 255.88 mbmp). **I)** *Operculodinium? longispinigerum* Matsuoka; central body length 34 μm (Lower Pliocene; 255.88 mbmp). **J)** *Operculodinium israelianum* (Rossignol); central body maximum diameter 61 μm (Lower Pliocene; 494.23 mbmp). **K)** *Tuberculodinium vancampoae* (Rossignol); maximum diameter 105 μm (Lower Pliocene; 476.40 mbmp). **L)** *Capisocysta lata* Head; maximum diameter 50 μm (Lower Pliocene; 477.04 mbmp). **M)** *Polysphaeridium zoharyi* (Rossignol); central body maximum diameter 58 μm (Lower Pliocene; 476.40 mbmp). **N)** *Selenopemphix quanta* (Bradford); central body maximum diameter 47 μm (Upper Pliocene; 234.12 mbmp). **O)** Typical palynofacies, after brief sonification and sieving at 10 μm, showing abundant fragmented micro-foraminiferal linings as darker subspherical objects, and lighter membranous debris of algal and possibly also foraminiferal origin. Note the virtual absence of terrigenous material. Length of field of view, 330 μm (Upper Pliocene; 226.01 mbmp).

dinoflagellate cysts/gram
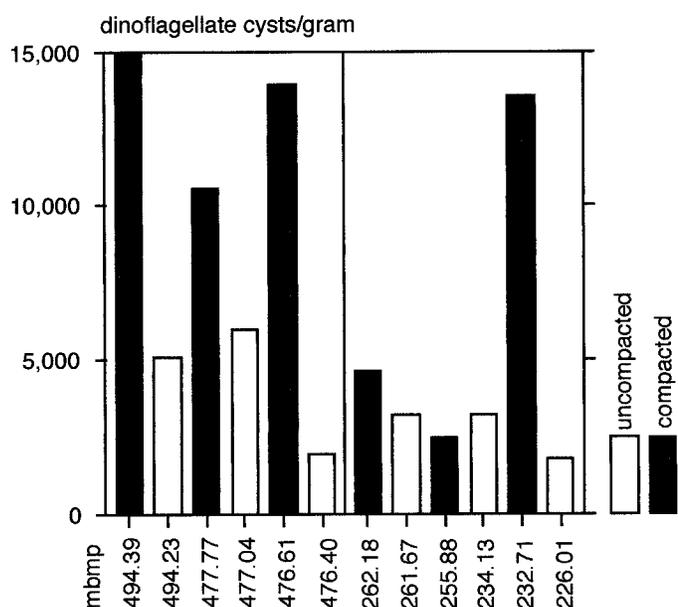
F_IG_. 7.—Concentrations of dinoflagellate cysts in compacted and uncompacted fine-grained Upper and Lower Pliocene samples (cf. Table 1). Note the distinctly higher numbers in most compacted samples, pointing to the passive enrichment of insoluble residue.

(2) Calcium-Carbonate Exporter Layers

The mechanical compaction of exporter layers is indicated by deformed peloids, their laminated appearance in thin section, and the presence of strongly flattened dinoflagellate cysts as seen under SEM. The slightly corroded appearance of the aragonite needles as seen in unetched broken surface samples (Fig. 5H) implies that the precursor sediment of the compacted layers in the shallow-burial environment must have been exposed to waters that led to dissolution of the metastable aragonite.

We propose that selective aragonite dissolution has taken place within the compacted layers during early diagenesis. Low-Mg calcite (microspar) was precipitated in the adjacent, now cemented, layers. The occurrence of pores that resemble the ''micro-vugs'' of Dix and Mullins (1988b) and Moshier (1989) suggests that dissolution of somewhat larger components also took place.

Lower Pliocene compacted layers consist mainly of loose, angular calcite grains of varying size (Fig. 5F$_2$). The smaller grains represent the calcitic residue concentrated by aragonite dissolution. The larger, angular calcite crystals apparently feature some later diagenetic overgrowth. The compacted layers are not protected against further compaction and dissolution because they lack a rigid cement framework. These layers will therefore undergo further mechanical compaction in later diagenesis. The diagenetic paths of compacted and uncompacted layers will continue to diverge. In samples from the Upper Pliocene section of the Clino core, the compacted layers still contain high amounts of aragonite (up to 85%; Fig. 5E). The process of mineral redistribution is obviously not yet completed. Nevertheless, the postulated end fabric of the dissolution path is a highly compacted limestone devoid of aragonite.

The distribution of aragonite in compacted versus uncompacted samples (Fig. 4) seems counterintuitive inasmuch as our model requires aragonite depletion of the compacted layers. The compacted samples show higher aragonite contents than the cemented samples. However, a compacted sediment that was highly aragonitic at the outset can remain proportionally rich in aragonite despite losing some of its aragonite during dissolution. In contrast, an uncompacted, originally aragonitic layer where calcite cement is precipitated will undergo a proportional decrease in aragonite by the import of calcite cement.

In Paleozoic successions the concept of alternating donor and receptor layers has been best documented for rhythmic limestone–marl alternations. On the basis of SEM studies and geochemical analyses in such alternations from the Silurian of Gotland, Munnecke and Samtleben (1996) and Munnecke (1997) showed that the marls, which are invariably mechanically compacted (discernibly by deformed ichnofossils and flattened acritarchs), represent an aragonite-depleted residual sediment. Aside from the primary aragonitic components, the fossil constituents of limestones and marls is strikingly similar. Thus, these authors assumed that the carbonate cement of the uncompacted limestones was provided by selective aragonite dissolution in the intercalated marls. The dissolved aragonite was transported diffusively and reprecipitated as calcite cement (microspar) in the limestone layers. A similar model of solution–reprecipitation in early diagenesis had been proposed by Eder (1982) for the Devonian and Carboniferous of Germany.

Because pressure and temperature conditions in the shallow-burial environment are insufficient to initiate mobilization of calcium carbonate at the burial depth in question for the cementation of uncompacted limestones, some other driving mechanism is required for initiating the redistribution processes. A possible mechanism is vertical gradients in pore-water chemistry. In the shallow-burial environment, geochemical gradients can result from microbial decomposition of organic matter (Canfield and Raiswell 1991). Such chemical gradients are able to cause aragonite dissolution close to the seafloor (e.g., Chilingar et al. 1967; Canfield and Raiswell 1991). Organic carbon (TOC) in the sediment samples from the Clino core is low in concentration, with an average of 0.19 wt % in the Lower Pliocene and 0.22 wt % in the Upper Pliocene (Westphal 1998). These values are at the lower end of the range typical for carbonates (Ricken 1993) and may explain why the diagenesis of these sediments appears incomplete. The difficulty in proving this connection is that the original TOC concentrations prior to diagenesis are unknown. The Pliocene succession from the Clino core could represent an immature stage in the development of a rhythmic lithographic limestone succession.

An enigma regarding differential rhythmic diagenesis is the trigger for the diagenetic alterations, especially where there are no discernible fluctuations in sediment input (Hallam 1986). It is well known that variations in sediment input usually influence the diagenetic development. Grain-size variations, for example, clearly lead to differences in the diagenetic patterns as seen in coarse-grained and fine-grained intervals from the Clino core (Westphal 1998; Melim et al. in press b). Mineralogic variations such as input fluctuations in the clay and carbonate contents also influence diagenetic development; for example, the fine-grained basinal periplatform sediments adjacent to the Great Bahama Bank show sediment-input cycles (Bernet et al. 1998). In the present study, none of the above variations could be unequivocally proven. Variations in sediment input that could be the cause of differential development in cemented and uncemented layers are not observed. With the methods applied here, including the integration of palynological data to detect subtle changes in the sediment input, the nature of the steering mechanism for the differential diagenesis remains unknown. This is largely because variations in the initial aragonite contents are poorly constrained owing to its metastability in this diagenetic environment. The absence of systematic variations in the palynologic record together with the uniform composition observed in thin sections nevertheless implies that the diagenetic differentiation is steered by factors other than sediment input variations, at least as detectable by our methods. Hence different diagenetic products appear to have developed from a similar precursor sediment.

CONCLUSIONS

(1) Rhythmic diagenesis in fine-grained aragonitic periplatform carbonates leads to the formation of alternating cemented and uncemented layers. Cementation takes place early, before accumulation of sedimentary overburden that would result in mechanical compaction. The uncemented layers, in contrast, are compacted.
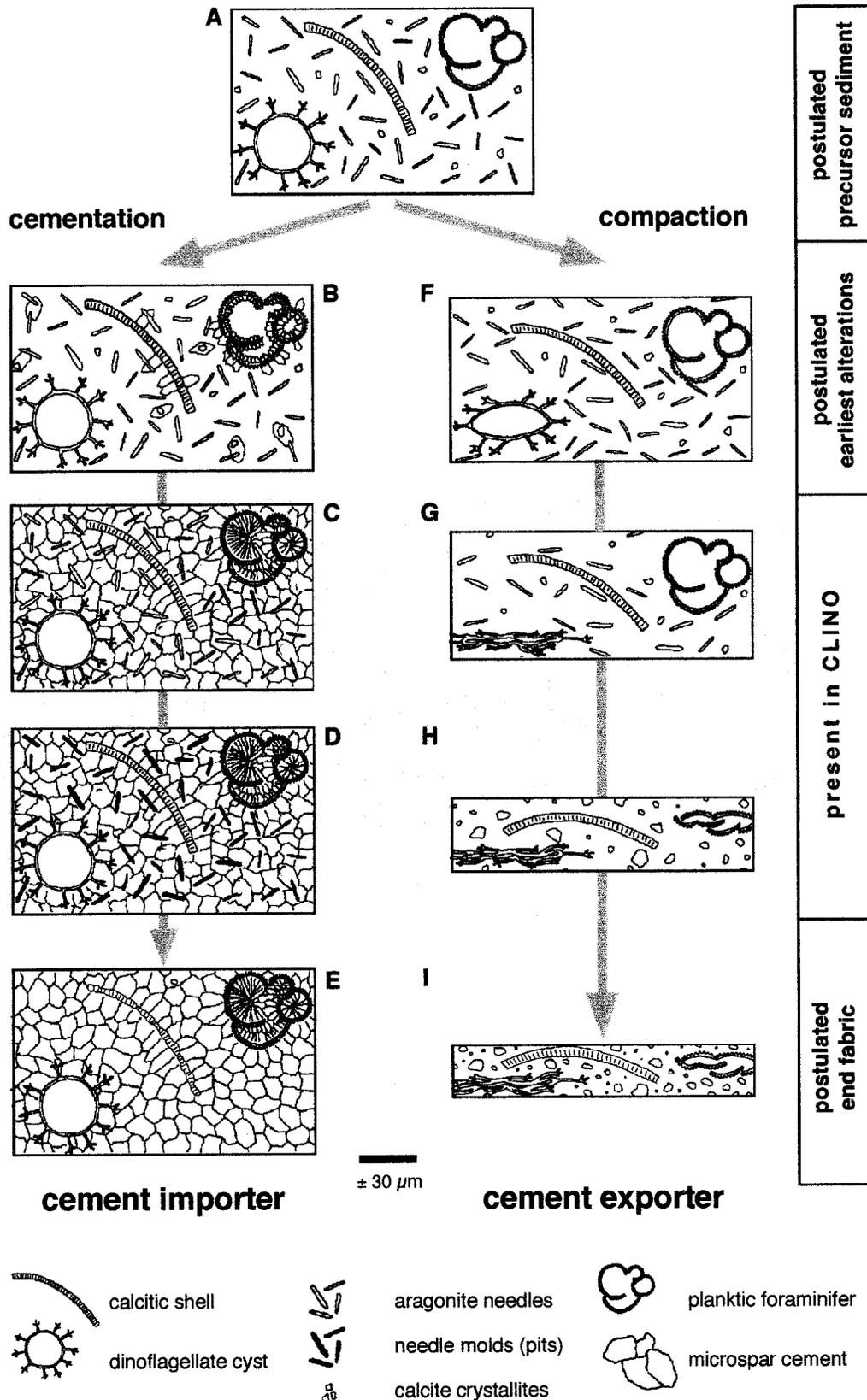
FIG. 8.—Diagenetic development of fine-grained, initially metastable carbonates in the marine shallow-burial environment. Left column: lithification path of the uncompacted cement importers. Right column: dissolution and compaction of the assumed source layers of the carbonate cement.

(2) There are no observable trends in the taxonomic composition of dinoflagellate cyst assemblages that would correlate with the development of uncompacted versus compacted layers. The sedimentary input as seen in thin section also appears very uniform. Our methods do not reveal any variations in sediment composition that might control the development of compacted and uncompacted intervals.

(3) On the basis of the assumed short distances traveled by solutes within sedimentary successions (Morse and Mackenzie 1993), and on petrographic observations, we propose that the carbonate cement observed in the uncompacted layers is sourced by the intercalated compacted layers. These two types of layers follow separate and distinct diagenetic paths that diverge from earliest diagenesis onward.

(4) The model proposed for the differential diagenesis of these pure limestone alternations is similar to models proposed for limestone–marl alternations (Eder 1982; Munnecke and Samtleben 1996). The pure limestone succession studied here can be understood as a clay-free analog to limestone–marl alternations.

REFERENCES

BATHURST, R.G.C., 1970, Problems of lithification in carbonate muds: Proceedings of the Geologists' Association, v. 81, p. 429–440.

BATHURST, R.G.C., 1971, Carbonate Sediments and Their Diagenesis: Amsterdam, Elsevier, Developments in Sedimentology, v. 12, 620 p.

BATHURST, R.G.C., 1987, Diagenetically enhanced bedding in argillaceous platform limestones: stratified cementation and selective compaction: Sedimentology, v. 34, p. 749–778.

BERNET, K.H., EBERLI, G.P., AND ANSELMETTI, F.S., 1998, The role of orbital precession in creating marl/limestone alternations, Neogene, Santaren Channel, Bahamas (abstract): International Association of Sedimentologists, 15th International Sedimentological Congress, Alicante, Spain, p. 191.

CANFIELD, D.E., AND RAISWELL, R., 1991, Carbonate precipitation and dissolution, in Allison, P.A., and Briggs, D.E.G., eds., Taphonomy: Releasing the Data Locked in the Fossil Record, New York, Plenum Press, p. 412–453.

CHILINGAR, G.V., BISSELL, H.J., AND WOLF, K.H., 1967, Diagenesis of carbonate rocks, in Larsen, G., and Chilingar, G.V., eds., Diagenesis in Sediments: Amsterdam, Elsevier, Developments in Sedimentology, v. 8, p. 179–322.

DIX, G.R., AND MULLINS, H.T., 1988a, A regional perspective of shallow burial diagenesis of deep-water periplatform carbonates from the northern Bahamas, in Austin, J.A., Schlager, W., et al., eds., Proceedings of the Ocean Drilling Program, Scientific Results, v. 101: College Station, Texas, p. 279–304.

DIX, G.R., AND MULLINS, H.T., 1988b, Rapid burial diagenesis of deep-water carbonates: Exuma Sound, Bahamas: Geology, v. 16, p. 680–683.

EBERLI, G.P., AND GINSBURG, R.N., 1987, Segmentation and coalescence of Cenozoic carbonate platforms, northwestern Great Bahama Bank: Geology, v. 15, p. 75–79.

EBERLI, G.P., AND GINSBURG, R.N., 1989, Cenozoic progradation of northwestern Great Bahama Bank, a record of lateral platform growth and sea-level fluctuations, in Crevello, P.D., Wilson, J.L., Sarg, J.F., and Read, J.F., eds., Controls on Carbonate Platform and Basin Development: SEPM, Special Publication 44, p. 339–351.

EBERLI, G.P., SWART, P.K., MCNEILL, D.F., KENTER, J.A.M., ANSELMETTI, F.S., MELIM, L.A., AND GINSBURG, R.N., 1997, A synopsis of the Bahama Drilling Project: Results from two deep core borings drilled on the Great Bahama Bank, in Eberli, G.P., Swart, P.K., and Malone, M.J., eds., Proceedings of the Ocean Drilling Program, Initial Reports, Leg 166: College Station, Texas, p. 23–41.

EDER, W., 1982, Diagenetic redistribution of carbonate, a process in forming limestone–marl alternations (Devonian and Carboniferous, Rheinisches Schiefergebirge, W. Germany), in Einsele, G., and Seilacher, A., eds., Cyclic and Event Stratification: Berlin, Springer-Verlag, p. 98–112.

EINSELE, G., AND RICKEN, W., 1991, Limestone–marl alternations—An overview, in Einsele, G., Ricken, W., and Seilacher, A., eds., Cycles and Events in Stratigraphy: Berlin, Springer-Verlag, p. 23–47.

ENOS, P., AND SAWATSKY, L.H., 1981, Pore networks in Holocene carbonate sediments: Journal of Sedimentary Petrology, v. 51, p. 961–985.

GINSBURG, R.N., ED., in press, Subsurface Geology of a Prograding Platform Margin, Great Bahama Bank: Results of the Bahamas Drilling Project: SEPM, Special Publication.

GOLDHAMMER, R.K., 1997, Compaction and decompaction algorithms for sedimentary carbonates: Journal of Sedimentary Research, v. 67, p. 26–35.

HALLAM, A., 1986, Origin of minor limestone–shale cycles: climatically induced or diagenetic?: Geology, v. 14, p. 609–612.

HEAD, M.J., AND WESTPHAL, H., 1999, Palynology and paleoenvironments of a Pliocene carbonate platform: the Clino Core, Bahamas: Journal of Paleontology, v. 73, p. 1–25.

KENTER, J.A.M., GINSBURG, R.N., AND TROELSTRA, S.R., in press, The Western Great Bahama Bank: Sea-level-driven sedimentation patterns on the slope and margin, in Ginsburg, R.N., ed., in press, Subsurface Geology of a Prograding Platform Margin, Great Bahama Bank: Results of the Bahamas Drilling Project: SEPM, Special Publication.

LASEMI, Z., AND SANDBERG, P.A., 1984, Transformation of aragonite-dominated lime muds to microcrystalline limestones: Geology, v. 12, p. 420–423.

LIDZ, B.H., AND MCNEILL, D.F., 1995, Reworked Paleogene to early Neogene planktic foraminifera: implications of an intriguing distribution at a late Neogene prograding margin, Bahamas: Marine Micropaleontology, v. 25, p. 221–268.

LIND, I., AND SCHIØLER, P., 1994, Dinoflagellate concentration as an independent reference for monitoring mineral mobilization in stylolites: Sedimentary Geology, v. 92, p. 53–65.

MAHER, L.J., 1981, Statistics for microfossil concentration measurements employing samples spiked with marker grains: Review of Palaeobotany and Palynology, v. 32, p. 153–191.

MELIM, L.A., 1996, Limitations on lowstand meteoric diagenesis in the Pliocene–Pleistocene of Florida and Great Bahama Bank: Implications for eustatic sea-level models: Geology, v. 24, p. 893–896.

MELIM, L.A., SWART, P.K., AND MALIVA, R.G., 1995, Meteoric-like fabrics forming in marine waters: Implications for the use of petrography to identify diagenetic environments: Geology, v. 23, p. 755–758.

MELIM, L.A., ANSELMETTI, F.S., AND EBERLI, G.P., in press a, The importance of pore type on permeability of Neogene carbonates, Great Bahama Bank, in Ginsburg, R.N., ed., in press, Subsurface Geology of a Prograding Platform Margin, Great Bahama Bank: Results of the Bahamas Drilling Project: SEPM, Special Publication.

MELIM, L.A., SWART, P.K., AND MALIVA, R.G., in press b, Meteoric and Marine Burial Diagenesis in the Subsurface of the Great Bahama Bank, in Ginsburg, R.N., ed., in press, Subsurface Geology of a Prograding Platform Margin, Great Bahama Bank: Results of the Bahamas Drilling Project: SEPM, Special Publication.

MORSE, J.W., AND MACKENZIE, F.T., 1993, Geochemical constraints on $CaCO_3$ transport in subsurface sedimentary environments: Chemical Geology, v. 105, p. 181–196.

MOSHIER, S.O., 1989, Microporosity in micritic limestones: a review: Sedimentary Geology, v. 63, p. 191–213.

MUNNECKE, A., 1997, Bildung mikritischer Kalke im Silur auf Gotland: Courier Forschungsinstitut Senckenberg, no. 198, 71 p.

MUNNECKE, A., AND SAMTLEBEN, C., 1996, The formation of micritic limestones and the development of limestone–marl alternations in the Silurian of Gotland, Sweden: Facies, v. 34, p. 159–176.

MUNNECKE, A., WESTPHAL, H., REIJMER, J.J.G., AND SAMTLEBEN, C., 1997, Microspar development during early marine burial diagenesis: a comparison of Pliocene carbonates from the Bahamas with Silurian limestones from Gotland (Sweden): Sedimentology, v. 44, p. 977–990.

PINGITORE, N.E., 1970, Diagenesis and porosity modification in Acropora palmata, Pleistocene of Barbados, West Indies: Journal of Sedimentary Petrology, v. 40, p. 712–721.

RICKEN, W., 1986, Diagenetic Bedding: A Model for Limestone–Marl Alternations: Berlin, Springer-Verlag, Lecture Notes in Earth Sciences, no. 6, 210 p.

RICKEN, W., 1993, Sedimentation as a Three-Component System: Lecture Berlin, Springer-Verlag, Lecture Notes in Earth Sciences, no. 51, 211 p.

SCHLANGER, S.O., AND DOUGLAS, R.G., 1974, The pelagic ooze–chalk–limestone transition and its implications for marine stratigraphy, in Hsü, K.J., and Jenkyns, H.C., eds., Pelagic Sediments on Land and Under the Sea: International Association of Sedimentologists, Special Publication 1, p. 117–148.

SCHMIDT, V., 1965, Facies, diagenesis, and related reservoir properties in the Gigas Beds (Upper Jurassic), Northwestern Germany, in Pray, L.C., and Murray, R.C., eds., Dolomitization and Limestone Diagenesis: Society of Economic Paleontologists and Mineralogists, Special Publication 13, p. 124–168.

STEINEN, R.P., 1982, SEM observations on the replacement of Bahaman aragonitic mud by calcite: Geology, v. 10, p. 471–475.

STOCKMARR, J., 1971, Tablets with spores used in absolute pollen analysis: Pollen et Spores, v. 13, p. 615–621.

WESTPHAL, H., 1998, Carbonate Platform Slopes—A Record of Changing Conditions. The Pliocene of the Bahamas: Berlin, Springer-Verlag, Lecture Notes in Earth Sciences, no. 75, 197 p.

WESTPHAL, H., REIJMER, J.J.G., AND HEAD, M.J., 1999, Input and diagenesis on a carbonate slope (Bahamas): response to morphology evolution and sea-level fluctuations, in Harris, P.M., Saller, A.H., and Simo, J.A., eds., Advances in Carbonate Sequence Stratigraphy—Application to Reservoirs, Outcrops, and Models: SEPM, Special Publication 63.